

The International Journal of Robotics Research

<http://ijr.sagepub.com>

On Path Planning and Obstacle Avoidance for Nonholonomic Platforms with Manipulators: A Polynomial Approach

Evangelos Papdopoulos, Ioannis Poulakakis and Iakovos Papdimitriou

The International Journal of Robotics Research 2002; 21; 367

DOI: 10.1177/027836402320556377

The online version of this article can be found at:
<http://ijr.sagepub.com/cgi/content/abstract/21/4/367>

Published by:

 SAGE Publications

<http://www.sagepublications.com>

On behalf of:



Multimedia Archives

Additional services and information for *The International Journal of Robotics Research* can be found at:

Email Alerts: <http://ijr.sagepub.com/cgi/alerts>

Subscriptions: <http://ijr.sagepub.com/subscriptions>

Reprints: <http://www.sagepub.com/journalsReprints.nav>

Permissions: <http://www.sagepub.com/journalsPermissions.nav>

Evangelos Papadopoulos

Department of Mechanical Engineering
National Technical University of Athens
Athens, Greece

Ioannis Poulakakis

Department of Mechanical Engineering
Centre for Intelligent Machines
McGill University
Montreal, Canada

Iakovos Papadimitriou

Department of Mechanical Engineering
University of California at Berkeley
Berkeley, CA, USA

On Path Planning and Obstacle Avoidance for Nonholonomic Platforms with Manipulators: A Polynomial Approach

Abstract

A planning methodology for nonholonomic mobile platforms with manipulators in the presence of obstacles is developed that employs smooth and continuous functions such as polynomials. The method yields admissible input trajectories that drive both the manipulator and the platform to a desired configuration and is based on mapping the nonholonomic constraint to a space where it can be satisfied trivially. In addition, the method allows for direct control over the platform orientation. Cartesian space obstacles are also mapped into this space in which they can be avoided by increasing the order of the polynomials employed in planning trajectories. The additional parameters required are computed systematically, while the computational burden increases linearly with the number of obstacles and the system elements taken into account. Illustrative examples demonstrate the planning methodology in obstacle-free and obstructed environments.

KEY WORDS—mobile manipulators, nonholonomic systems, obstacle avoidance, path planning, pfaffian constraints

1. Introduction

Mobile manipulator systems, consisting of a mobile platform equipped with one or more manipulators, are of great importance to a host of applications, mainly due to their ability to reach targets that are initially outside of the manipulator reach. Applications for such systems abound in mining, construc-

tion, forestry, planetary exploration and the military. A wide category of such systems employs wheeled mobile robots, which is the type of system under study in this paper.

Wheeled mobile robots have attracted a lot of interest recently. Work in the area can be divided into work on *wheeled mobile platforms* and work on *mobile manipulator systems*, i.e., manipulators mounted on wheeled mobile platforms. Research on wheeled mobile platforms typically concentrates on motion planning, obstacle avoidance and platform navigation in cluttered environments. Research on the latter mostly focuses on techniques for motion planning of the integrated system in the absence of obstacles or deals with effects due to the coupling between the manipulator and its mobile platform.

Motion planning for mobile platforms is concerned with obtaining open loop controls, which steer a platform from an initial state to a final one, without violating the nonholonomic constraints. The idea of employing piecewise constant inputs to generate motions in the directions of iterated Lie brackets has been exploited by Lafferriere and Sussmann (1991), while Gurvitz (1992) developed planning tools based on averaging theory, where high amplitude high frequency control inputs have been used to approximate a holonomic collision-free path within a predetermined bound. Fliess et al. (1997) used the notion of a flat nonlinear system in motion planning for a car with n trailers. Murray and Sastry (1993) used sinusoids at integrally related frequencies to steer systems in power or chained form. In contrast to this approach, Monaco and Normand-Cyrot (1992) used multirate digital control and a family of piecewise constant inputs. A comprehensive survey of developments in control of nonholonomic systems can be found in Kolmanovsky and McClamroch (1995).

The above methods do not take explicitly under consideration obstacles in the workspace. Many algorithms have been proposed for solving this problem for wheeled mobile platforms. These can be roughly categorized into search-based methods, geometric approaches and probabilistic approaches. Barraquand and Latombe (1991) used an exhaustive search-based method that explores the system's configuration space by propagating step motions corresponding to some controls. In most of the geometric methods, the final path computed by a planner is the concatenation of elementary paths computed by a basic procedure. Jacobs and Canny (1989) define a set of canonical trajectories, which satisfy the constraints, such as straight-line segments followed by arc segments. Laumond et al. (1994) use the same families of canonical trajectories to transform a path, calculated by a geometric planner that ignores the motion constraints, into a feasible one. To overcome the problem of discontinuous curvature profiles of the paths resulting from the above planners, Sheuer and Fraichard (1997) used a set of paths called *bi-elementary paths*, which are composed by arcs of *clothoids*. Fleury et al. (1995) used combinations of *clothoids* and *anticlothoids* to replace a collision free trajectory, consisting of straight directed line segments, by a smooth, time optimal one. An alternative approach for solving the problem of obstacle avoidance utilizes probabilistic learning methods. Svestka and Overmars (1994) proposed a learning approach, where the motion planning process is split into a learning phase, in which a probabilistic roadmap is constructed in the configuration space, and a query phase, in which this roadmap is used to find paths between different pairs of configurations. The approach can be extended to both normal car-like robots and car-like robots that move only forward by using suitable local methods for computing paths that are feasible for the robot. Other approaches include dynamic programming techniques, progressive constraints (Ferbach 1995), least square approximation of a path returned by a holonomic planner based on artificial force fields (Bemporad, De Luca, and Oriolo 1996), minimizing cusps number (Shkel and Lumelsky 1997), and obstacle traversal (Shiller 2000).

The above methods cannot be applied in general classes of nonholonomic systems, because the admissible paths are not known *a priori*. To the best of our knowledge, the most general result is due to Sekhavat and Laumond (1998). The authors show how the algorithm developed in Laumond et al. (1994) can be extended for a class of nonholonomic systems that are or can be transformed into *chained form*. The basic idea lies in replacing the optimal trajectories (linear segments and circular arcs) with a family of canonical trajectories computed by any local planner respecting some topological property.

A host of issues related to *mobile manipulator systems* has been studied in the past. These include dynamic and static stability (Papadopoulos and Rey 1996), force development and application (Papadopoulos and Gonthier 1999), control in the presence of compliance (Hootsmans and Dubowsky 1991), dynamic coupling issues (Wiens 1989), etc. However,

in these studies, the mobile manipulator platform is assumed to be stationary.

Moving mobile manipulator systems present many unique problems that are due to the coupling of holonomic manipulators with nonholonomic bases. Seraji (1998) presents a simple on-line approach for motion control of mobile manipulators using augmented Jacobian matrices. The approach is kinematic and requires additional constraints to be met for the manipulator configuration. Perrier et al. (1998) represent the nonholonomy of the vehicle as a constrained displacement and try to make the global feasible displacement of the system correspond to the desired one. Foulon et al. (1999) consider the problem of task execution by coordinating the displacements of a nonholonomic platform with a robotic arm using an intuitive planner, where a transformation, similar to the one proposed in Section 3, was presented. The same authors introduce other variations of local planners, which are then combined to constitute a generalized space planner (Foulon, Fourquet, and Renaud 1998). Papadopoulos and Poulakakis (2000b) presented a planning and control methodology for mobile manipulator systems allowing them to follow desired end-effector and platform trajectories simultaneously without violating the nonholonomic constraints.

The problem of navigating a mobile manipulator among obstacles has been studied by Yamamoto and Yun (1995) by simultaneously considering the obstacle avoidance problem and the coordination problem. The developed controller allows the system to retain optimal or sub-optimal configurations while the manipulator avoids obstacles using potential functions. In their approach, they assume that only the manipulator and not the platform may encounter the obstacle, while Tanner and Kyriakopoulos (2000) studied the problem of obstacle avoidance by the entire mobile manipulator system. Their nonholonomic motion planner is based on a discontinuous feedback law under the influence of a potential field.

In this paper, a planning and obstacle avoidance methodology is developed for nonholonomic platforms with manipulators. The developed method uses smooth and continuous functions such as polynomials and it is computationally inexpensive and easy to apply. The method constructs trajectory inputs that drive both the manipulator and its platform to a final configuration without violating the nonholonomic constraint. The idea employed is to construct a transformation that maps the nonholonomic constraint associated with a given platform point from the Cartesian space to a space where it can be satisfied trivially. The proposed transformation is obtained through a systematic methodology that can also be applied directly to other more complex systems. Since the mapping is smooth and planning in this new space is achieved using polynomial trajectories, the resulting Cartesian paths and trajectories are also smooth. Due to the specific map chosen, the method allows for direct control over the platform orientation.

The developed transformation also maps Cartesian space obstacles to transformed ones produced by length and shape preserving transformations. Obstacle avoidance is achieved by increasing the order of the polynomials that are used in planning trajectories. Enclosing general obstacles in simple shapes such as ellipses or circles facilitates computation of the additional parameters required, while computations are of algebraic nature. Taking into account all of the vertices and edges of a mobile system guarantees collision avoidance for the entire system, while the computational burden increases linearly with the number of obstacles and system elements. Extensive use of the method showed that it is particularly suitable for applications in open environments where the workspace of the robot is not highly cluttered by obstacles, e.g., outdoor applications, or planetary exploration operations. Due to its inherent algebraic nature, the scheme proposed significantly reduces the number of computations required to solve the problem with the tradeoff of a possible miss of a solution in a highly cluttered environment. Illustrative examples demonstrate the application of the methodology in obstacle-free and obstructed spaces.

2. Mobile Manipulator System Kinematics

A prerequisite for the successful use of mobile manipulators is the availability of a planning methodology that can generate feasible paths for driving the end effector to the desired coordinates without violating system nonholonomic constraints. However, in many applications, it is required that the platform position and orientation are also specified for a number of reasons. Such reasons include the particular site geometry or ground morphology, the avoidance of manipulator joint limits or singularities, the mating of the system to a given port, and the maximization of a system's manipulability or force output. Moreover, the calculated paths must be computationally inexpensive to compute and should be able to steer the system away from obstacles, which may exist in its workspace.

Because nonholonomy is associated with the mobile platform, while the manipulator is holonomic, the system is studied as two connected subsystems, the holonomic manipulator and its nonholonomic platform. This allows one to find an admissible path for the mobile platform that can drive it from an initial position and orientation to a final desired one. Next, using known techniques for manipulators, joint trajectories are calculated for the manipulator so that its end-effector is driven to its destination. An advantage of this approach is that it is very simple to extend the method to mobile systems with multiple manipulators on board.

For simplicity reasons, we concentrate here on a mobile system, which consists of a two degree-of-freedom (DoF) manipulator mounted on a differentially driven mobile platform (see Figure 1). However the developed methodology can be applied equally well to systems with N DoF manipulators, or

to car-like mobile platforms (Papadopoulos and Poulakakis 2000).

2.1. Holonomic Manipulator Subsystem

The Cartesian coordinates of the end effector E relative to the world frame are given by (see Figure 1)

$$x_E = x_F + l_1 \cos(\varphi + \vartheta_1) + l_2 \cos(\varphi + \vartheta_1 + \vartheta_2) \quad (1)$$

$$y_E = y_F + l_1 \sin(\varphi + \vartheta_1) + l_2 \sin(\varphi + \vartheta_1 + \vartheta_2), \quad (2)$$

where (x_F, y_F) is the position of the manipulator mounting point F on the mobile platform, φ is the platform orientation, ϑ_1 and ϑ_2 represent the joint angles and l_1 and l_2 denote the link lengths of the manipulator arms. Note that, although the motion of the manipulator is holonomic, point F of the platform is still subject to a nonholonomic constraint, as it will be discussed later.

Inversion of eqs (1) and (2) is easy and yields equations of the form

$$\vartheta_1 = \vartheta_1(x_E, y_E, x_F, y_F, \varphi) \quad (3)$$

$$\vartheta_2 = \vartheta_2(x_E, y_E, x_F, y_F) \quad (4)$$

that compute the joint angles ϑ_1 and ϑ_2 which correspond to some end-effector position (x_E, y_E) when the platform position (x_F, y_F) and orientation φ are known.

The existence of a solution requires that

$$\begin{aligned} |l_1 - l_2| \leq \|EF\| \leq l_1 + l_2 &\Rightarrow (l_1 - l_2)^2 \\ &\leq (x_E - x_F)^2 + (y_E - y_F)^2 \leq (l_1 + l_2)^2. \end{aligned} \quad (5)$$

If the above inequality is not satisfied at some point, then the target is outside the manipulator reach, and the mobile platform must move.

2.2. Nonholonomic Mobile Platform Subsystem

The mobile platform employs two independently driven wheels (see Figure 1). Here it is assumed that the speed at which the system moves is low and therefore the two driven wheels do not slip sideways. Hence, the velocity of any point G on the wheel axis is normal to this axis. This leads to following constraint equation:

$$\dot{x}_G \sin \varphi - \dot{y}_G \cos \varphi = 0. \quad (6)$$

Equation (6) is a nonholonomic constraint involving velocities and, as is well known, it cannot be integrated analytically to result in a constraint between the configuration variables of the platform, namely, x_G , y_G , and φ . Also, the configuration space of this system is three-dimensional (completely unrestricted) while the velocity space is two-dimensional. In general, it can be shown that any point P on the platform that

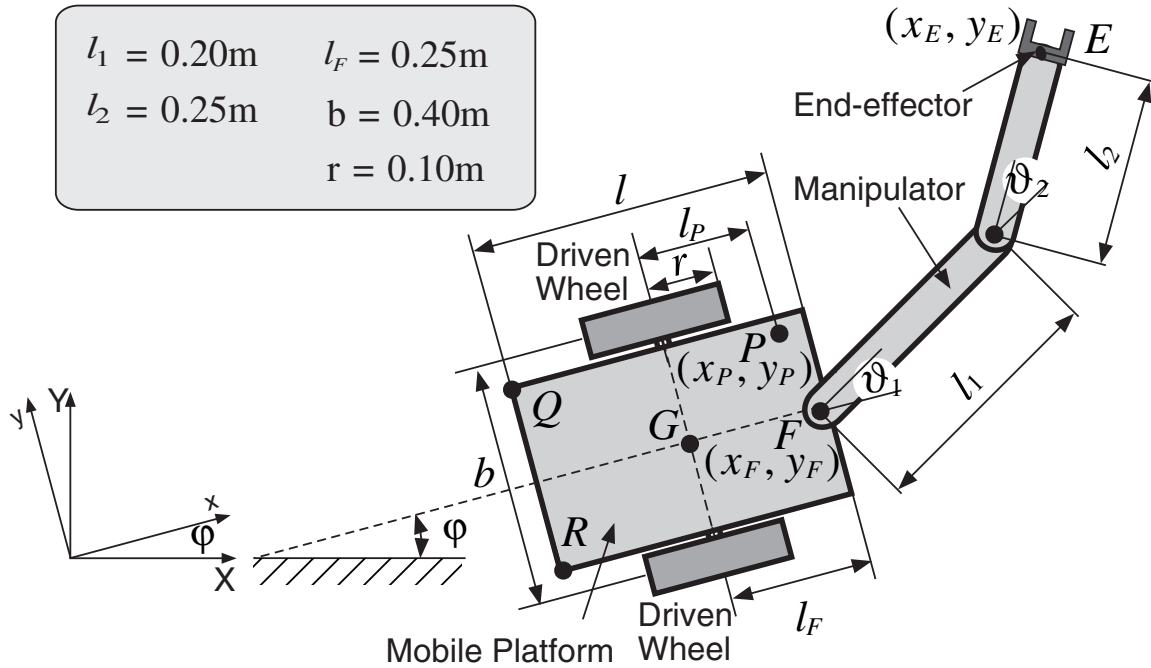


Fig. 1. Mobile manipulator system on a differentially-driven platform.

moves with it and is away from the wheel axis, is subjected to the following constraint:

$$\dot{x}_P \sin \varphi - \dot{y}_P \cos \varphi + \dot{\varphi} l_P = 0, \tag{7}$$

where l_P is the normal distance between the point and the axis of the wheels. For the manipulator mounting point F , in particular, eq (7) applies by replacing the index P with F .

Finally, if the platform motion to a destination is known and described by the trajectory of some point, for example point F , then it is relatively simple to relate platform control variables, namely the angular velocities of the left and right wheels, $\dot{\vartheta}_\ell$ and $\dot{\vartheta}_r$, to point velocities, (\dot{x}_F, \dot{y}_F) , and platform angular velocity, $\dot{\varphi}$. This relationship is given by

$$\begin{bmatrix} \dot{x}_F \\ \dot{y}_F \\ \dot{\varphi} \end{bmatrix} = \begin{bmatrix} \frac{r}{2} \cos \varphi + \frac{l_{Fr}}{b} \sin \varphi & \frac{r}{2} \cos \varphi - \frac{l_{Fr}}{b} \sin \varphi \\ \frac{r}{2} \sin \varphi - \frac{l_{Fr}}{b} \cos \varphi & \frac{r}{2} \sin \varphi + \frac{l_{Fr}}{b} \cos \varphi \\ -\frac{r}{b} & \frac{r}{b} \end{bmatrix} \begin{bmatrix} \dot{\vartheta}_\ell \\ \dot{\vartheta}_r \end{bmatrix}, \tag{8}$$

where all parameters are defined in Figure 1. As shown by eq (8), the two control angular rates, $\dot{\vartheta}_\ell$ and $\dot{\vartheta}_r$, are mapped to three output velocities.

3. Path Planning

A mobile system is especially useful when the manipulator task is outside the manipulator's reach. Assuming that this

is the case, we focus our attention in finding a path for the mobile platform, which connects its initial configuration as described by $(x_F^{in}, y_F^{in}, \varphi^{in})$ to a final one $(x_F^{fin}, y_F^{fin}, \varphi^{fin})$. It is well known that this problem is not trivial, since one must satisfy the nonholonomic constraint and achieve a change in the three dimensional configuration space with two controls only. Next, a planning methodology is developed that allows for a systematic approach of nonholonomic constraints of the form of eq (7).

To describe the motion of the platform, one must choose a point. Among platform points, point G , the middle of the wheel axis and F , the manipulator mounting point, can be candidate due to their location on the platform. For reasons that will be discussed later, point F is chosen here. The constraint given by eq (7) is scleronomic and can be written for point F in the Pfaffian form

$$P(x_F, y_F, \varphi) dx_F + Q(x_F, y_F, \varphi) dy_F + R(x_F, y_F, \varphi) d\varphi = 0, \tag{9a}$$

with

$$\begin{aligned} P(x_F, y_F, \varphi) &= \sin \varphi, Q(x_F, y_F, \varphi) \\ &= -\cos \varphi, R(x_F, y_F, \varphi) = l_F. \end{aligned} \tag{9b}$$

Note that eq (9) contains three differentials. Such constraints also appear in other systems of engineering interest,

such as space free-floating systems, or legged systems in free-flight (Papadopoulos and Dubowsky 1991). Therefore, planning motions for systems that are subjected to such constraints have interest beyond the area of wheeled platforms.

As will be shown by the end of this section, planning can be facilitated if this form is transformed to one in which only two differentials appear. This is indeed possible because it is known (Pars 1965) that nonintegrable Pfaffian equations of the form of eq (9a) can be written as

$$du + vd w = 0, \tag{10}$$

where u, v, w are properly selected functions of x_F, y_F , and φ .

Equation (9a) can be transformed into eq (10), if the following equations hold:

$$P = \frac{\partial u}{\partial x_F} + v \frac{\partial w}{\partial x_F}, \quad Q = \frac{\partial u}{\partial y_F} + v \frac{\partial w}{\partial y_F}, \tag{11}$$

$$R = \frac{\partial u}{\partial \varphi} + v \frac{\partial w}{\partial \varphi}.$$

To find the unknown functions u, v , and w , we construct the differential equations that they must satisfy. To this end, we define the following auxiliary functions:

$$P' = \frac{\partial Q}{\partial \varphi} - \frac{\partial R}{\partial y_F}, \quad Q' = \frac{\partial R}{\partial x_F} - \frac{\partial P}{\partial \varphi}, \tag{12}$$

$$R' = \frac{\partial P}{\partial y_F} + v \frac{\partial Q}{\partial x_F}.$$

Substitution of eq (11) into eq (12) yields

$$P' = \frac{\partial v}{\partial \varphi} \frac{\partial w}{\partial y_F} - \frac{\partial v}{\partial y_F} \frac{\partial w}{\partial \varphi}, \quad Q' = \frac{\partial v}{\partial x_F} \frac{\partial w}{\partial \varphi} - \frac{\partial v}{\partial \varphi} \frac{\partial w}{\partial x_F}, \tag{13}$$

$$R' = \frac{\partial v}{\partial y_F} \frac{\partial w}{\partial x_F} - \frac{\partial v}{\partial x_F} \frac{\partial w}{\partial y_F}.$$

Multiplying P' by $\partial w/\partial x_F$, Q' by $\partial w/\partial y_F$, and R' by $\partial w/\partial \varphi$, respectively, and adding the results yields the following differential equation for w :

$$P' \frac{\partial w}{\partial x_F} + Q' \frac{\partial w}{\partial y_F} + R' \frac{\partial w}{\partial \varphi} = 0. \tag{14}$$

Similarly, multiplying P' by $\partial v/\partial x_F$, Q' by $\partial v/\partial y_F$, and R' by $\partial v/\partial \varphi$, respectively, and adding the results, yields the following differential equation for v :

$$P' \frac{\partial v}{\partial x_F} + Q' \frac{\partial v}{\partial y_F} + R' \frac{\partial v}{\partial \varphi} = 0. \tag{15}$$

Therefore, both w and v satisfy the same first order partial differential equation, i.e., any solution to eq (14) is also a solution to eq (15).

Finally, multiplying P' by $P - \partial u/\partial x_F$, Q' by $Q - \partial u/\partial y_F$, and R' by $R - \partial u/\partial \varphi$, adding the results, and using eqs (11) and (14) yields

$$\left(P - \frac{\partial u}{\partial x_F}\right) P' + \left(Q - \frac{\partial u}{\partial y_F}\right) Q' + \left(R - \frac{\partial u}{\partial \varphi}\right) R' = v \left(P' \frac{\partial w}{\partial x_F} + Q' \frac{\partial w}{\partial y_F} + R' \frac{\partial w}{\partial \varphi}\right) = 0. \tag{16}$$

Therefore, u satisfies the following differential equation:

$$P' \frac{\partial u}{\partial x_F} + Q' \frac{\partial u}{\partial y_F} + R' \frac{\partial u}{\partial \varphi} = P P' + Q Q' + R R' \neq 0. \tag{17}$$

The right hand side in the above equation does not vanish, because the condition of integrability is not satisfied. If the system were holonomic, then u would have satisfied the same differential equation as v and w .

Next, the partial differential equation, eq (14), is solved to yield w . The general solution is any function of the two independent integrals of the subsidiary system (Ince 1956),

$$\lambda(x_F, y_F, \varphi) = x_F \cos \varphi + y_F \sin \varphi = k_1 \tag{18a}$$

$$\mu(x_F, y_F, \varphi) = \varphi = k_2, \tag{18b}$$

where k_1 and k_2 are arbitrary real numbers. Of those functions, a useful choice is

$$w = \mu(x_F, y_F, \varphi) = \varphi = k_2, \tag{19}$$

because this solution allows control over the platform orientation, while simplifying the resulting planning and obstacle avoidance equations. Other choices exhibit different properties that may be useful in meeting other requirements.

Equation (19) represents a solution to the linear partial differential equation given by eq (14). Note that in this case no particular solution can be selected because no boundary conditions have been imposed. Hence, eq (19) holds for all $k_2 \in \mathbf{R}$.

Equation (9a), in view of eqs (11) and (19), yields

$$P dx_F + Q dy_F + R d\varphi = \frac{\partial u}{\partial x_F} dx_F + \frac{\partial u}{\partial y_F} dy_F + \frac{\partial u}{\partial \varphi} d\varphi = du = 0, \tag{20}$$

i.e., for any particular value k_2 of w eq (9a) is a perfect differential. Next, a solution for u is obtained by integration of eq (20) under the constraint imposed by eq (19). Note that eq (20) would be meaningless if eq (19) did not hold. Indeed, eq (19) forms an algebraic constraint among the variables, which holds for every k_2 , and is used to find u by expressing φ and $d\varphi$ with respect to the other variables and k_2 . Here, we

simply have $\varphi = k_2$ and $d\varphi = 0$. Substitution of these into eq (20) results in a perfect differential

$$dh(x_F, y_F, k_2) = \sin k_2 dx_F - \cos k_2 dy_F = 0. \quad (21)$$

Integration of eq (21) yields

$$h(x_F, y_F, k_2) = x_F \sin k_2 - y_F \cos k_2 = \text{const.} \quad (22)$$

Equations (21) and (22) hold for every $k_2 \in \mathbf{R}$. Replacing k_2 by $\mu(x_F, y_F, \varphi) = \varphi$, the function $u(x_F, y_F, \varphi)$, i.e., a solution to eq (17) results:

$$u(x_F, y_F, \varphi) = x_F \sin \varphi - y_F \cos \varphi. \quad (23)$$

Hence, expressions for u and w have been found. The expression for v is found using any of eqs (11). Choosing the last one yields

$$v(x_F, y_F, \varphi) = l_F - x_F \cos \varphi - y_F \sin \varphi. \quad (24)$$

Summarizing, the nonholonomic constraint described by eq (9) can be written in the form given by eq (10) if

$$u(x_F, y_F, \varphi) = x_F \sin \varphi - y_F \cos \varphi \quad (25a)$$

$$v(x_F, y_F, \varphi) = l_F - x_F \cos \varphi - y_F \sin \varphi \quad (25b)$$

$$w(x_F, y_F, \varphi) = \varphi. \quad (25c)$$

Equations (25) constitute a transformation $(x_F, y_F, \varphi) \rightarrow (u, v, w)$, which is defined at every point of the configuration space of the system. As will be seen in Section 4, this property is a prerequisite when it comes to obstacle avoidance, since it allows for mapping of obstacles in the Cartesian x - y space into the u - v - w space without singularities. Moreover, the orientation φ of the platform is conserved through the transformation as a chain coordinate, and is explicitly available for planning, i.e., one can directly set a desired trajectory for φ , and therefore avoid undesirable cusps. A similar coordinate transformation was proposed in Foulon, Fourquet, and Renaud (1999), where it was derived from direct reasoning based on the kinematics of point G . However, as mentioned above, finding a transformation for point F greatly facilitates the computation of paths for obstacle avoidance.

This transformation is very helpful for planning purposes. Indeed, if we choose functions f and g as follows:

$$w = f(t) \quad (26)$$

$$u = g(w) \quad (27)$$

$$v = -\frac{du}{dw} = -g'(w), \quad (28)$$

then eq (10) is satisfied identically. Therefore, the planning problem reduces to choosing functions f and g such that they satisfy the initial and final configuration variables. Such functions can be polynomials, splines, or any other continuous and

smooth time function. In particular, f can be any function of time whose value at initial and final time is equal to the initial and final platform orientation. Shaping f during the motion allows complete control over the orientation and therefore, motions with undesired orientation changes are avoided.

Function g is constructed using similar functions and eqs (25a) and (25b) for computing the initial and final values for u and v , respectively. Finally, v , which requires a simple differentiation, is computed using eq (28). Once u , v , and w have been found, the platform coordinates are computed by inverting eqs (25). Elimination of time among these yields the desired platform path and orientation that, if followed, the platform will be driven to the desired final location and orientation, without violating the constraint. The manipulator joint motion is then computed using eqs (3) and (4). Since the method requires algebraic manipulation of polynomials and a single differentiation, it is computationally inexpensive and yields results rapidly.

Example 1. To illustrate the methodology described above, we employ the mobile manipulator system shown in Figure 1. The main task for the system is to have the end-effector reach a desired target point with coordinates (x_E, y_E) , while the platform point F must reach a desired position and orientation, (x_F, y_F, θ) . Assuming that the platform can be steered to its destination, the holonomic inverse relations, eqs (3) and (4), can be used to compute the manipulator final joint values.

In order to compute platform trajectories, functions f and g in eqs (26)-(28) are selected to be fifth and third order time polynomials, respectively,

$$f(t) = a_5 t^5 + a_4 t^4 + a_3 t^3 + a_2 t^2 + a_1 t + a_0$$

$$g(w) = b_3 w^3 + b_2 w^2 + b_1 w + b_0.$$

The coefficients of polynomial f are computed using the initial and final orientation, angular velocity and angular acceleration of the platform (Ince 1956). The coefficients of polynomial g satisfy the initial and final conditions of the Cartesian motion, as computed using eqs (25a) and (27), while its derivatives at the boundaries are computed using eqs (25b) and (28).

For the simulation, the total move time is chosen equal to 6 s and the initial configuration is $(x_E^{in}, y_E^{in}, x_F^{in}, y_F^{in}, \varphi^{in}) = (0.35 \text{ m}, 0.3 \text{ m}, 0 \text{ m}, 0.5 \text{ m}, -90^\circ)$. Using eqs (3) and (4), the initial posture of the manipulator is found to be $(\vartheta_1^{in}, \vartheta_2^{in}) = (39.7^\circ, 46.5^\circ)$. The final desired configuration is $(x_E^{fin}, y_E^{fin}, x_F^{fin}, y_F^{fin}, \varphi^{fin}) = (1.1 \text{ m}, 2.35 \text{ m}, 1 \text{ m}, 2 \text{ m}, -90^\circ)$ and the corresponding final manipulator joint angles are $(\vartheta_1^{fin}, \vartheta_2^{fin}) = (-46.6^\circ, 70.27^\circ)$. Note that choosing a different total time will make the system move faster or slower, but will have no effect on the Cartesian path of the mobile platform.

Figure 2 depicts snapshots of the motion of the mobile manipulator, while Figure 3 depicts the corresponding trajectories for platform and manipulator joint velocities. It can

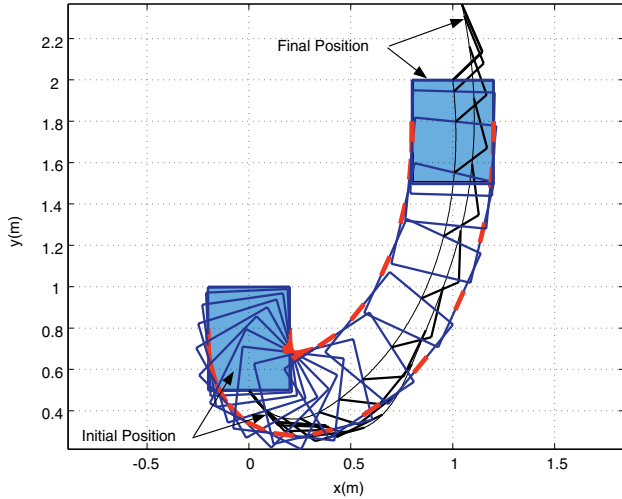


Fig. 2. Motion animation of the mobile manipulator system.

be observed that both the system path and trajectories are smooth, and drive the system from its initial configuration to the desired one in the specified time.

If we examine the method used closer, we observe that the orientation of the platform changes according to its trajectory, while the system moves so that it reaches its destination at the given time. This method will always work as described with the exception of equal initial and final vehicle orientation with simultaneous zero initial and final angular velocities and accelerations. In this case, the vehicle is required to stay on a straight line and therefore it cannot reach all points in the Cartesian space. A straightforward solution to this problem is to use a via point, or even better, to add a multiple of a full turn, (360°), either at the initial or at the final vehicle orientation.

4. Obstacle Mapping

A planning methodology is more useful if it allows the construction of paths that can avoid proximal obstacles. In this section, we study how general Cartesian obstacles are mapped through the transformation given by eqs (25), and then concentrate on obstacles that can be enclosed in ellipses or circles. In the next section, we focus on constructing paths that avoid them. It is assumed that the location of obstacles in the proximal system workspace is known and fixed.

Equations (25) map obstacles in the Cartesian x - y space into the u - v - w space. Mapping from a two dimensional to a three dimensional space adds one dimension which, in this case, corresponds to the orientation of the platform. To study the properties of the developed transformation, eqs (25) are written in matrix form

$$\begin{bmatrix} u \\ v \\ w \\ 1 \end{bmatrix} = \begin{bmatrix} \sin \varphi & -\cos \varphi & 0 & 0 \\ -\cos \varphi & -\sin \varphi & 0 & l_F \\ 0 & 0 & 1 & 0 \\ 0 & 0 & 0 & 1 \end{bmatrix} \begin{bmatrix} x_F \\ y_F \\ \varphi \\ 1 \end{bmatrix}, \quad (29)$$

where the determinant of the above matrix is always nonzero. Therefore, this transformation constitutes a global diffeomorphism in the configuration space. Further decomposition of eq (29) using the product of two matrices yields

$$\begin{bmatrix} u \\ v \\ w \\ 1 \end{bmatrix} = \begin{bmatrix} 1 & 0 & 0 & 0 \\ 0 & -1 & 0 & 0 \\ 0 & 0 & 1 & 0 \\ 0 & 0 & 0 & 1 \end{bmatrix} \begin{bmatrix} \cos(\pi/2 - \varphi) & -\sin(\pi/2 - \varphi) & 0 & 0 \\ \sin(\pi/2 - \varphi) & \cos(\pi/2 - \varphi) & 0 & -l_F \\ 0 & 0 & 1 & 0 \\ 0 & 0 & 0 & 1 \end{bmatrix} \begin{bmatrix} x_F \\ y_F \\ \varphi \\ 1 \end{bmatrix} \quad (30)$$

$$\mathbf{u} = \mathbf{T}_1 \mathbf{T}_2 \mathbf{x}$$

where matrix \mathbf{T}_1 corresponds to a reflection and matrix \mathbf{T}_2 to a rotation by $\pi/2 - \varphi$ and a translation by $-l_F$.

It is known that transformations such as rotations, translations and reflections, preserve both the length and the shape of an object. These properties are crucial for mapping obstacles from the Cartesian x - y space to the transformed space. However, since the map is a function of the orientation φ , a single object in the Cartesian space is mapped to a family of such objects that correspond to the range of φ that is considered. For example, a linear segment in the Cartesian x - y space is transformed to a family of linear segments in the u - v - w space having the same length as the original segment and orientation, which depends on the current orientation φ of the platform. This is an important observation because many obstacles are either polygonal, or can be enclosed in polygons, i.e., closed sequences of linear segments.

To construct a simple and fast trajectory planner that can avoid obstacles, it is assumed that obstacles can be enclosed in an ellipse or a circle depending on the obstacle's shape. This approach simplifies the definition of the distance between an obstacle and the mobile system, due to the symmetry properties of these basic shapes. For example, Figure 4 depicts an elliptic and a circular obstacle in the Cartesian x - y space. These are transformed to the obstacles depicted in Figure 5.

It can be seen that, for all $w = \varphi$, the obstacles in the u - v - w space are still an ellipse and a circle, while the centers of both families of obstacles lie on helicoids. Appendix A gives examples of analytical expressions for the transformed obstacles.

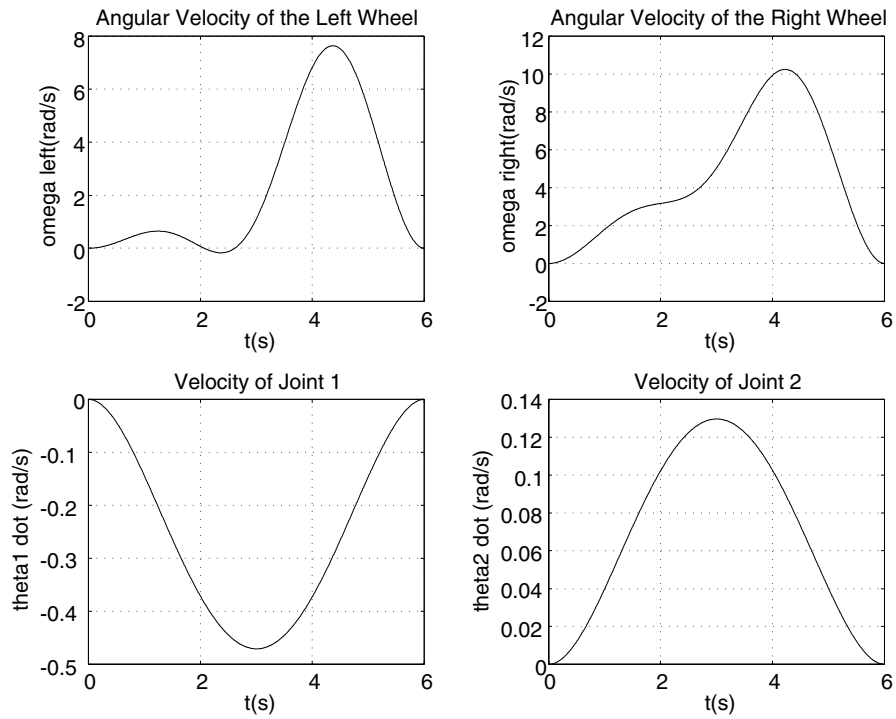


Fig. 3. Rate trajectories for the mobile manipulator system inputs.

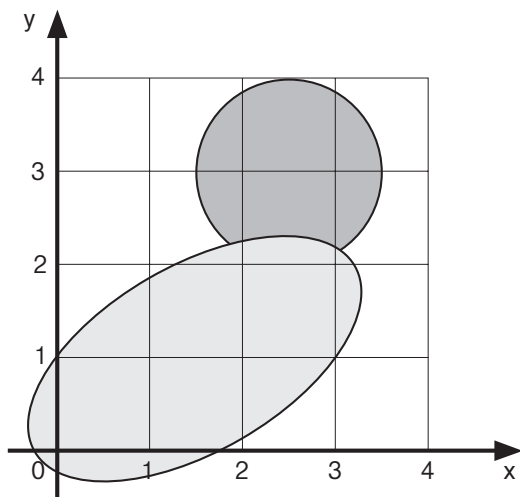


Fig. 4. Obstacles in the Cartesian x - y space.

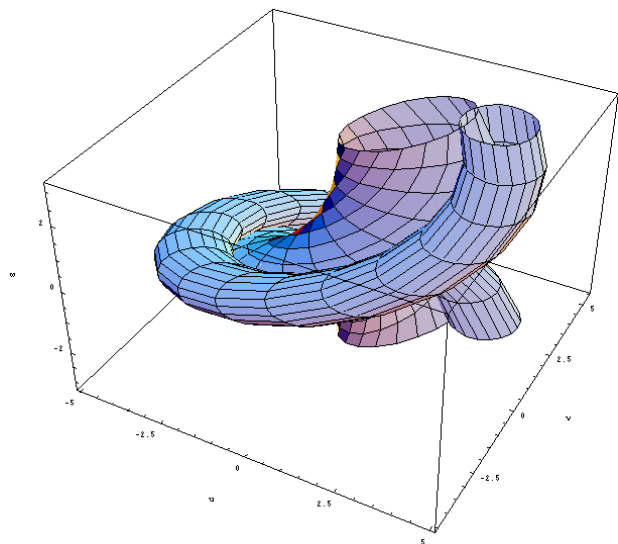


Fig. 5. The obstacles in Figure 4 transformed in the u - v - w space.

5. Obstacle Avoidance Principle

The planning method developed above did not take into account obstacles, which may exist in the workspace. It is obvious that, to avoid an obstacle, additional freedom must be introduced in the planning scheme.

A simple way to achieve this is to introduce additional coefficients in the polynomial $u(w)$ whose number may depend on the number of the obstacles and their positions in the workspace. These additional coefficients should not affect the satisfaction of the initial and final conditions but should allow one to shape the path in the u - v - w space so as to avoid collisions with the obstacles. In this way, the problem of avoiding Cartesian obstacles can be reduced to the problem of finding appropriate values for the additional coefficients. Due to the nature of the involved equations this is a much simpler problem, and results in a simple analytical solution without the use of intensive numerical searches.

As an example of the use of the method, the case of a single platform point and a single obstacle is studied first. The case of collision avoidance for the full mobile manipulator system in the presence of multiple obstacles is treated in the next section.

5.1. Single Obstacle

A single obstacle is assumed and a single additional coefficient b_4 is added to the polynomial $u(w)$. Since the nonholonomic constraint must be satisfied everywhere, the following equations for u and v must hold:

$$u(w) = b_4 w^4 + \sum_{i=0}^3 b_i w^i \tag{31}$$

$$v(w) = -4b_4 w^3 - \sum_{i=1}^3 i b_i w^{i-1}. \tag{32}$$

Introducing the initial and final conditions for u and w which correspond to the initial and final positions for point F of the platform, the following linear system is obtained with respect to the unknown coefficients $b_i, i = 0, \dots, 3$:

$$\sum_{i=0}^3 b_i w_{in}^i = u(w_{in}) - b_4 w_{in}^4 \tag{33}$$

$$\sum_{i=0}^3 b_i w_{fin}^i = u(w_{fin}) - b_4 w_{fin}^4 \tag{34}$$

$$\sum_{i=1}^3 i b_i w_{in}^{i-1} = -v(w_{in}) - 4b_4 w_{in}^3 \tag{35}$$

$$\sum_{i=1}^3 i b_i w_{fin}^{i-1} = -v(w_{fin}) - 4b_4 w_{fin}^3. \tag{36}$$

Solving the above system, the $b_i, i = 0, \dots, 3$, are found as linear functions of b_4 . Therefore, eqs (31) and (32) along with the solution of eqs (33)-(36) yield the polynomials u and v , which satisfy the constraint and the initial and final conditions as functions of the additional coefficient b_4 . By changing the value of b_4 , different paths satisfying the desired boundary conditions are obtained. The problem reduces to finding a range of values of b_4 which lead to paths that avoid the obstacle. This is done next, assuming that the obstacle is contained in either a circle or an ellipse.

For an obstacle enclosed in a circle, centered at (x_0, y_0) with radius R , the distance between the center of the obstacle and some point P of the platform must be greater than the radius R . Making use of the fact that a circular obstacle is mapped in the u - v - w space onto a circle of the same radius, then for each $w = \varphi$ and for collision avoidance, the following inequality must hold:

$$(u(w) - u_0(w))^2 + (v(w) - v_0(w))^2 > R^2 \tag{37}$$

$$\forall w \in [w_{in}, w_{fin}],$$

where $u(w)$ and $v(w)$ are the transformed coordinates of point P on the mobile system and $u_0(w)$ and $v_0(w)$ are the transformed coordinates of the center of the obstacle for the corresponding orientation $w = \varphi$. Similarly, for an ellipse centered at (x_0, y_0) , rotated at an angle ψ and with principal axes lengths R_a and R_b , the criterion for obstacle avoidance is that for each $w = \varphi$ the following inequality must hold true:

$$R_b^2 [(u(w) - u_0) \cos \psi' - (v(w) - v_0) \sin \psi']^2 + R_a^2 [(u(w) - u_0) \sin \psi' + (v(w) - v_0) \cos \psi']^2 - R_a^2 R_b^2 > 0. \tag{38}$$

Substituting eqs (31) and (32) into eq (37) for the case of a circular obstacle and eqs (31) and (32) into eq (38) for the case of an elliptic obstacle and after some algebraic manipulations, the following inequality is obtained:

$$\alpha b_4^2 + \beta b_4 + \gamma > 0. \tag{39}$$

The coefficients α, β , and γ are different for circles and ellipses. However, in both cases they are known functions of w and of $u_{in}, v_{in}, w_{in}, u_{fin}, v_{fin}, w_{fin}$. Equation (39) is a very practical representation of the criterion for obstacle avoidance. If this inequality holds for all $w = \varphi$, then the planned path will never collide with the obstacle.

Notice that because eq (39) is a distance criterion and because all $b_i, i = 0, \dots, 3$, are linear functions of b_4 , the resulting inequality will always be a second order polynomial in b_4 . In addition, as shown in Appendix B, the coefficient α is always a non-negative number, and therefore satisfaction of eqs (37)-(38) requires that b_4 lies outside of the roots $b_4^a(w), b_4^b(w)$ of the second order polynomials in eq (39). This fact

greatly simplifies the problem of finding the appropriate values of b_4 for which eqs (37)-(38) are satisfied and is a direct result of the chosen transformation, given by eqs (25). Indeed, these values are found by simple algebraic operations and therefore, this methodology is very fast to compute.

Example 2. To illustrate the avoidance methodology, point F is chosen to represent the motion of the platform. The path in Figure 2 is assumed to encounter a circular obstacle with center at $(x_0, y_0) = (1.2 \text{ m}, 0.9 \text{ m})$ and radius $R = 0.25 \text{ m}$. To satisfy the inequality given by eq (39), the roots of the second order polynomial are plotted and shown in Figure 6. For w greater than approximately 32° the polynomial has two real roots $b_4^a(w), b_4^b(w)$, at 32° it has two equal roots, and below this value, it has no roots. Inside the locus in Figure 6, the distance criterion is not satisfied, i.e., there is a collision with the obstacle. If one chooses $b_4 = 0$, then the path that will result will collide with the obstacle and the angle at which it will collide will be approximately 42° .

As shown in Figure 6, to make sure that the resulting path will not collide with the obstacle, one must choose a b_4 in the range $(-0.08, -\infty)$ which defines the admissible region for b_4 . A specific value in this region can be selected according to some criterion such as the minimum difference from the unobstructed path, or the minimum path length. Figure 7 depicts the modified system path that corresponds to $b_4 = -0.15$.

The resulting path avoids the obstacle although it remains close to the initial one. Figure 7 clearly shows that, to avoid the obstacle, the mobile system moves initially backwards, while in the case of Figure 2, the platform moves forward. The corresponding input trajectories are still smooth and given in Figure 8.

5.2. Extension to Multiple Obstacles

The above method can be easily extended to the case in which multiple obstacles exist and are enclosed in circular or elliptic shapes. In this case, several inequalities of the form of eq (39) must be satisfied, each representing a distance from an obstacle.

In the case of N obstacles, the following inequalities for b_4 must hold:

$$\alpha_{i4}b_4^2 + \beta_{i4}b_4 + \gamma_{i4} > 0, \quad i = 1, \dots, N. \quad (40)$$

Since $\alpha_{i4} > 0$ for $w \in (w_{in}, w_{fin})$, the same methodology used for a single obstacle can be used here. Therefore, an additional obstacle requires no more than an additional call to a routine of algebraic nature that uses the same equations with different obstacle coordinates and shape. The range of admissible b_4 will be possibly smaller than for one obstacle.

If one coefficient cannot lead to the calculation of an obstacle free path then three alternative techniques can be employed. The simplest two include the use of intermediate points and the addition of 360° to the initial or final orientation so as to give more freedom to the planning scheme.

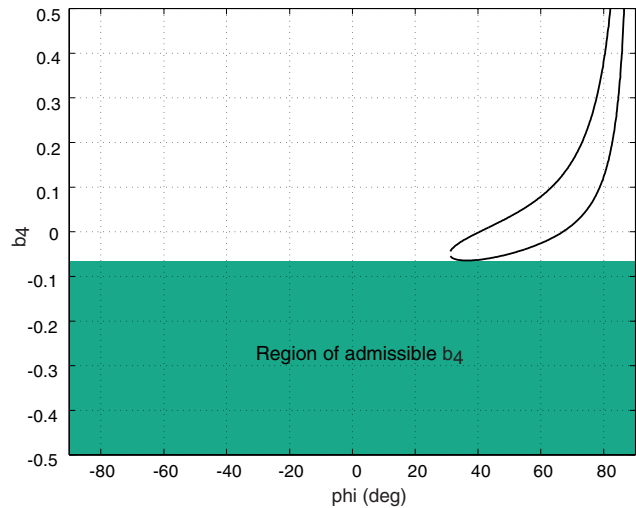


Fig. 6. Admissible range for b_4 in the presence of a single obstacle.

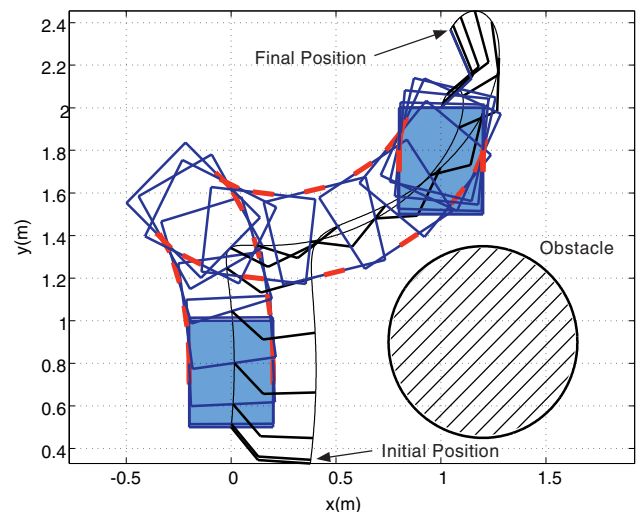


Fig. 7. Modified path that avoids the obstacle.

If these techniques cannot produce a path, then an additional coefficient b_5 can be used. However, in that case the computation of the admissible regions of the additional coefficients is more complicated. The above techniques are currently under investigation.

6. Generalization of the Method

As stated earlier, the method developed in the previous section ensures that the front point of the platform will not collide with some obstacle but does not take into account other platform

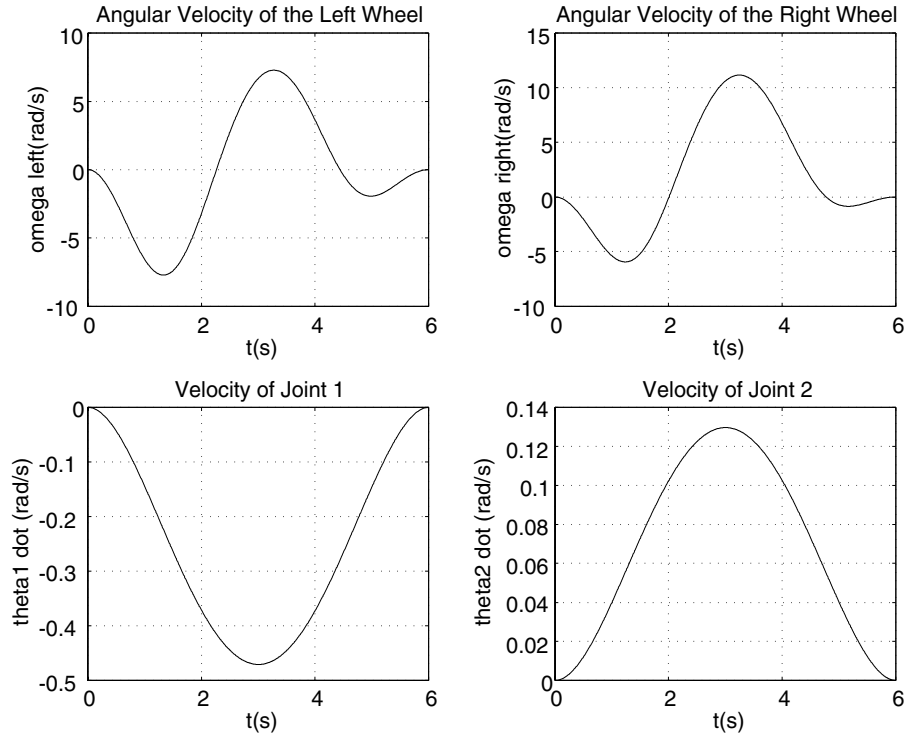


Fig. 8. Input rate trajectories the path shown in Figure 7.

points and the manipulator. A simple technique to account for these is to use a safety length, l_{cr} , so as to make sure that, when the selected control point does not collide, then the whole mobile system will not collide either. This technique will work fine when the obstacles are not cluttered compared to the dimensions of the system.

Although such a technique is very easy to implement, it is quite conservative. Therefore, in this section the developed method is extended to allow elimination of collisions between obstacles and the mobile system itself. This requires that platform and manipulator vertices and edges are taken into account. The basic idea is to map these elements to the $u-v-w$ using the transformation described by eqs (25) and appropriate collision avoidance criteria.

As an example of mapping a vertex, point R on the platform is examined (see Figure 1). The $(x-y-\varphi) \rightarrow (u-v-w)$ transformation yields

$$w_R = w_F = w \tag{41a}$$

$$u_R(w) = u_F(w) + \frac{b}{2} \tag{41b}$$

$$v_R(w) = v_F(w) + l \tag{41c}$$

where l is the length of the platform. Equations (41) connect point R with point F and can be used for any other point on

the platform. Note that these equations are particularly simple and they only require addition of the relative displacements of point R with respect to point F , namely $b/2$ and l . Substituting eqs (41) into the obstacle avoidance criterion, eq (37) or eq (38), results again in a second order polynomial in b_4 , which may restrict the range of admissible values for b_4 .

The calculation of admissible values for b_4 for platform edges and manipulator links is considered next. Here, the requirement for no collision is that no such element becomes tangent to an obstacle. Since the manipulator desired joint trajectories are known *a priori*, all manipulator link point positions are written as functions of the known joint variables and of platform positions and orientations to be determined. Therefore, platform edges and manipulator links are treated similarly. As an example of an edge map, platform edge RQ is considered (see Figure 1). Edge points are transformed according to

$$u(w) = u_F(w) + d, d \in [-b/2, b/2] \tag{42}$$

$$v(w) = v_F(w) + l, \tag{43}$$

where d is a variable that denotes the lateral distance of each point of the segment RQ from the midpoint of the platform. Assuming a circular obstacle, the distance criterion that must be satisfied to avoid collisions is

$$(u_F(w) + d - u_0(w))^2 + (v_F(w) + l - v_0(w))^2 > R^2 \tag{44}$$

where $w \in [w_{in}, w_{fin}]$ and $d \in [-b/2, b/2]$. After some algebraic manipulations, the above inequality reduces to

$$h(d) = \alpha d^2 + \beta d + \gamma > 0, \tag{45}$$

$$d \in [-b/2, b/2]$$

where coefficients α , β , and γ are known functions of b_4 , w and of the boundary conditions $u_{in}, v_{in}, w_{in}, u_{fin}, v_{fin}, w_{fin}$. Equation (45) represents the distance between the center of a circle and any point on the infinite line, on which the line segment RQ lies. It is thus obvious that coefficient α is expected to be positive (as shown in Appendix B) for both circular and elliptic obstacles. Indeed, function $h(d)$ attains its minimum value at a point located at a lateral distance $d = -\beta/2\alpha$ on the line along RQ . This minimum value corresponds to the normal distance between the line and the center of the circle. Positive α denotes the fact that there is always a part of the infinite line that is located outside the circle. Therefore, the goal is to have the specific line segment RQ ($d \in [-b/2, b/2]$) lie outside the obstacle. In other words, eq (45) must not have any real roots for all $d \in [-b/2, b/2]$, i.e.,

$$\beta^2 - 4\alpha\gamma < 0, \text{ for } d \in [-b/2, b/2]. \tag{46}$$

The left side of Inequality (46) is in fact a second order polynomial in b_4 whose coefficients are known functions of w and of the boundary conditions. Selecting a value for b_4 that satisfies this inequality for every w ensures a collision-free path.

More specifically, as shown in Appendix B, the coefficient of the second order monomial in eq (46) is always negative. Therefore, by switching the inequality sign and the signs of the coefficients, the procedure for finding the range of b_4 that satisfies eq (46) becomes similar to the one described in Section 5.

The roots of the polynomial, calculated for all w , yield the range of b_4 for which the infinite line, on which the platform edge lies, becomes tangent to the obstacle. To restrict the criterion to the points on the line segment RQ only, i.e., for $d \in [-b/2, b/2]$, the algorithm first calculates the roots b_4 of the polynomial in eq (46) for some w and then substitutes them in the minimum distance expression, $d = -\beta/2\alpha$. This checks which point of the infinite line is tangent to the circle. For example, if this $d(b_4)$ is computed to be between $[-b/2, b/2]$, then the tangency point indeed lies on the platform edge (line segment RQ) and therefore the calculated root b_4 results in a tangency of RQ with the obstacle. Else, the tangency point is beyond the boundaries of the edge RQ and thus the calculated root b_4 is discarded. In this way, only the range

of b_4 which results in a tangency between RQ and the obstacle is taken into account. Selecting a value for b_4 outside this range ensures a collision-free path.

To completely avoid mobile system collisions with all obstacles, the tasks described above are completed for all platform edges and manipulator links, and for every obstacle in the proximal workspace. For the manipulator, as mentioned earlier, first its joint trajectories are computed and subsequently are incorporated in the polynomial coefficients, as constant values for each w . In all cases, the equations involved are always of analytic second-order polynomial nature, while the number of operations increases linearly with the number of elements and obstacles involved in the avoidance checks.

Example 3. The mobile system and the initial and final configurations of Example 2 are used in conjunction with three obstacles, shown in Figure 9. Plotting the roots of the second order polynomials in eq (39) for point F only results in Figure 10.

Next, the entire mobile manipulator system is taken into account. Manipulator joint trajectories are planned using 5th order polynomials, whose coefficients are such that they satisfy the initial and final conditions of motion, i.e., angular position, velocity and acceleration requirements. Applying the generalized method, a new range of admissible values for the coefficient b_4 is found and is depicted in Figure 11. More specifically, for each obstacle, the roots of second order polynomials for all platform vertices and manipulator joints, as well as platform edges and manipulator links, are calculated and plotted. Admissible values for b_4 are those that lie outside the roots of all the polynomials. As previously, all computations are straightforward and of algebraic nature.

Comparing Figure 11 with Figure 10, it is evident that the acceptable region for b_4 has been restricted substantially.

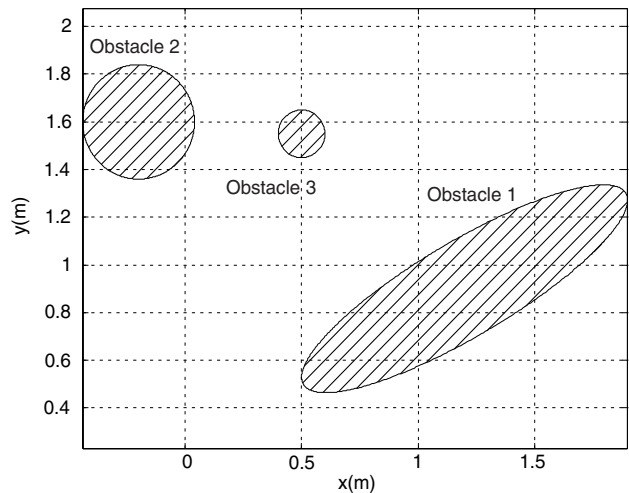


Fig. 9. Distribution of multiple obstacles in the workspace.

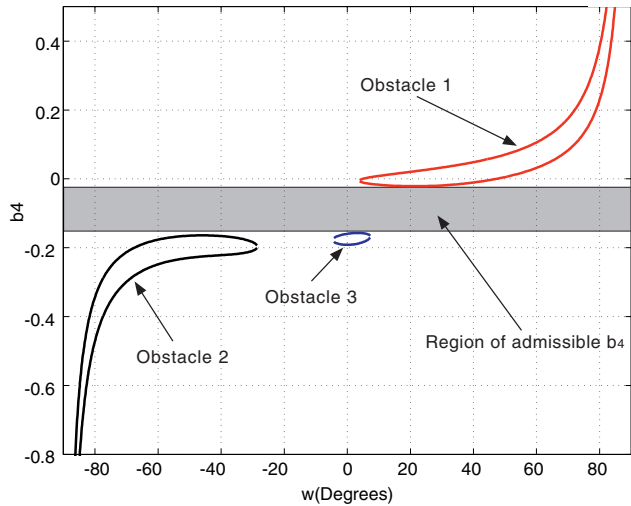


Fig. 10. Region of admissible b_4 s for the three obstacles in Figure 9 and point F .

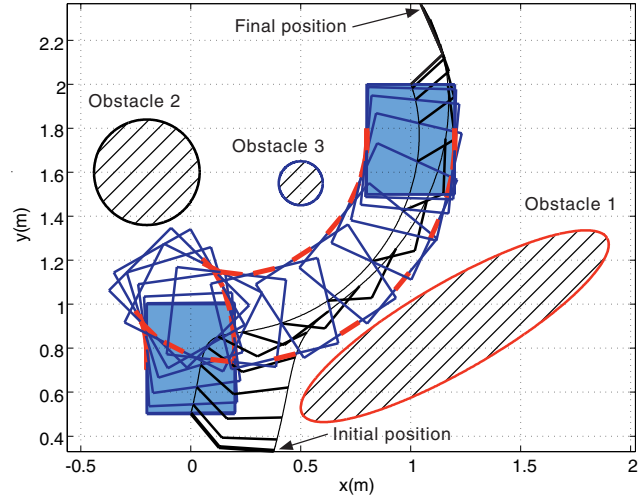


Fig. 12. Modified path that avoids the three obstacles completely.

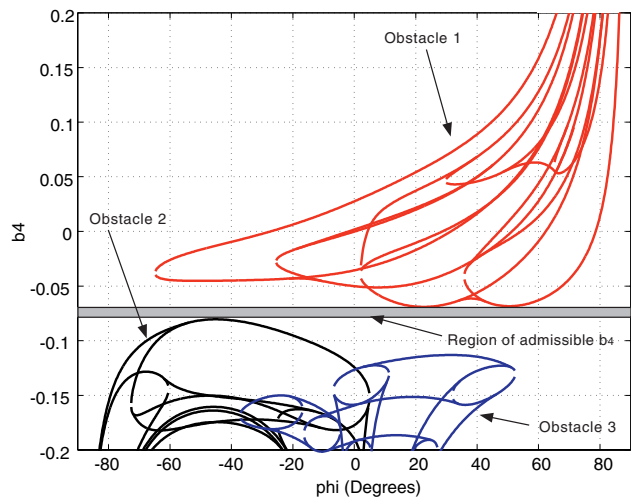


Fig. 11. Restricted region of admissible b_4 for the three obstacles in Figure 9.

By selecting $b_4 = -0.075$, the path shown in Figure 12 is obtained and, as expected, the entire system avoids all obstacles. The corresponding system input trajectories are shown in Figure 13.

As shown in Figure 12, the resulting path is smooth with a continuous curvature profile. Figure 13 shows that input trajectories are also smooth, and require no excessive velocities, while the mobile system starts and stops smoothly.

7. Discussion and Remarks

After having presented the planning and obstacle avoidance method, some important issues regarding its use are addressed. The first one is related to the selection of the particular transformation, eqs (25), used for the planning and obstacle avoidance method developed in this paper. Other transformations, derived by direct reasoning based on the kinematics of point G , could have been used as well. One of the simplest and classical transformations is discussed below. It is shown that its use introduces additional complexity especially when obstacle avoidance is considered. Therefore, although one could in principle derive an alternative transformation very easily, this does not necessarily result in an easy to implement obstacle avoidance technique.

Choosing point G in a constraint involving two differentials, see eq (6), and if $\varphi \neq (2k + 1)\pi/2$, division by $\cos \varphi$ yields a constraint of the form of eq (10). Then, the following transformation can be readily obtained:

$$u = y_G, v = -\tan \varphi, w = x_G, \tag{47}$$

$$\varphi \neq (2k + 1)\pi/2$$

and the methodology developed earlier, can result in planning and obstacle avoidance. However, use of eq (47) results in drawbacks that limit its effectiveness.

First, using this transformation does not yield bounded polynomial coefficients for $g(w)$ if the starting or ending orientation is $\varphi = (2k + 1)\pi/2$, or if the x coordinate of G does not change (Craig 1989). To avoid these problems, the coordinate system must be changed, so that the transformation given by eq (47) holds. In addition, this method fails to change the orientation of the platform if the initial and final location of

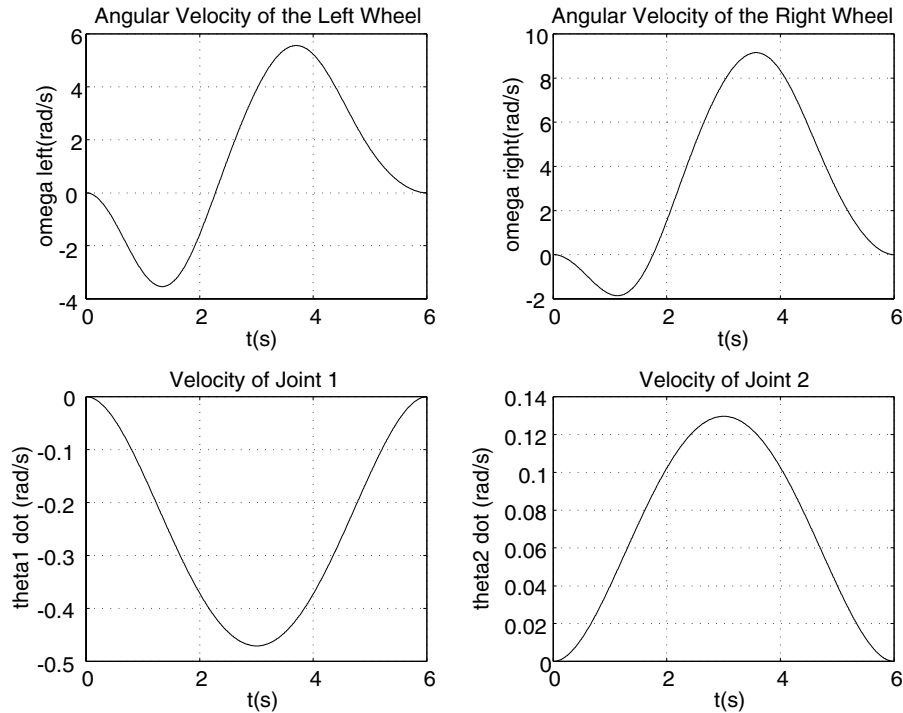


Fig. 13. Input rate trajectories for the path shown in Figure 12.

G are the same. To do this, especially in the case of a car-like system, an intermediate (via) point for G must be introduced.

Although these shortcomings can be addressed with some additional burden, more serious problems appear when it comes to obstacle avoidance. To avoid an obstacle, distances from system vertices and edges must be calculated. However, all these distances except the ones for point G include the angle φ :

$$\begin{aligned} u_p &= y_p = y_G + f_1(\varphi), \\ w_p &= x_p = x_G + f_2(\varphi). \end{aligned} \tag{48}$$

Since φ is not conserved through the transformation, distance inequalities become very complex and nonlinear functions of b_4 , with multiple solution branches. Solving for the valid range of b_4 requires use of numerical root solvers, which drastically increase the computational burden and may fail to yield a complete range.

In contrast to these shortcomings, the transformation given by eqs (25) gives complete control over the platform orientation φ , it is valid everywhere and the polynomials $f(t)$ and $g(w)$ can be defined always, except when the initial and final orientation are the same. As noted earlier, this is handled very easily by adding a multiple of a full turn to either the initial or final orientation. Also, since φ is conserved as a chained coordinate, and since both u and v are linear functions of

b_4 , then all distance criteria are second order polynomials of b_4 with coefficients that are available analytically. Therefore, computing the valid range of coefficients b_4 is much simpler and faster than in the case where eqs (47) are used.

Another important aspect of the use of the developed method is its behavior and its limitations with respect to the number, shape and location of the obstacles. In all cases, the existence of a valid range of b_4 depends on the shape of the curves in the b_4 - w plane. A single obstacle results in a single curve which either consists of bounded and closed branches, like the one that corresponds to obstacle 3 in Figure 10, or of two branches that tend to infinity, like the ones that correspond to obstacles 1 and 2 in the same figure. The first type of curve poses no problem to planning because both branches are contained between two values of b_4 and therefore they always leave an infinite range of valid coefficients b_4 . The other type of curve requires a closer examination.

Inspection of the expression for α (see eq (B1)) shows that $\alpha = 0$ only when $w = w_{in}$ or $w = w_{fin}$. Therefore, infinite roots may appear only at the initial or the final platform orientation. Computing analytically γ for $w = w_{in}$ or $w = w_{fin}$, it is easy to see that γ is negative only in the trivial cases where the initial or final (desired) position for the system's point under consideration is inside an obstacle. In those cases, the roots of the polynomial in eq (39) are infinite and of different signs, hence no valid range for b_4 exists, as expected. In all

other cases, infinite roots, if they appear, are all of the same sign. This being the case, then even if infinite roots appear either at $w = w_{in}$ or at $w = w_{fin}$, a valid range for b_4 exists. If they appear at both $w = w_{in}$ and $w = w_{fin}$ and are all of the same sign, again a valid range occurs. Therefore, the only case in which no valid range may appear is when the infinite roots at $w = w_{in}$ and $w = w_{fin}$ are of different signs and the invalid regions overlap.

Although it is difficult to analytically find when this may occur, extensive simulations and reasoning showed that this may happen when the system is very close to an obstacle and the initial motion, given the required evolution of the orientation $\varphi = w$ is such that drives the system towards the obstacle, whatever the value of the b_4 is. By similar reasoning, the same can occur when one considers the destination point and the inverse motion to the initial location. Such cases were indeed identified. However, in all cases, the mere addition of a full turn, either at the initial orientation or at the final one, did produce a valid range for b_4 . The relatively large margin in $\varphi = w$ allows for driving of the system to its destination without difficulty. Therefore, we may conclude that in the case of a single obstacle, the developed methodology always has a solution.

The observations derived from a single object can be extrapolated to the case of many obstacles. Each obstacle contributes an additional curve that may restrict the range of valid coefficients. As mentioned earlier, if no valid b_4 can be computed, then one may use via points or additional platform turns. These techniques increase the range of possible vehicle maneuvers and therefore tend to yield viable paths.

It should be noted here that it is not possible to exclude the possibility that the method will not find a path in a highly cluttered environment with confined passages, even if such a path exists. However, it has the advantage of quickly yielding a path for many environments with low obstacle density. Indeed, a very important property of the proposed method is that the number of operations increases linearly with the number of elements and obstacles involved in the avoidance checks. Treating an additional obstacle requires knowledge of its geometry and location only. Other than that, all equations remain the same and are analytically known and of algebraic nature; an additional obstacle requires an additional call to a fast algebraic routine. This is clearly an advantage of the method against heavy cell-decomposition approaches where the computational burden is high, and can be used in cases where a fast planning solution under low computational burden is a requirement.

8. Conclusions

In this paper, a novel planning methodology has been developed for nonholonomic mobile platforms with manipulators in the presence of obstacles that uses smooth and continuous

functions such as polynomials. The method yields admissible input trajectories that drive both the manipulator and the platform to a final configuration and is based on mapping the nonholonomic constraint to a space where it can be satisfied trivially. Because it requires algebraic manipulations and a single differentiation, implementation of the method is computationally inexpensive, while it allows direct control over the platform orientation. The resulting paths and trajectories are smooth due to the nature of the map and to the use of smooth polynomials.

It was shown that the developed transformation also maps Cartesian space obstacles to families of transformed ones. Obstacle avoidance for a system element requires that the path in the transformed space does not collide with the obstacle's image. This was achieved by increasing the order of the polynomials that were used in planning. Enclosing general obstacles in simple shapes such as ellipses or circles facilitates computation of the additional parameters required. The method allows for checking avoidance for all vertices and edges of the mobile system and hence collisions of the system with obstacles can be avoided. Due to its inherent algebraic nature, the scheme proposed here significantly reduces the number of computations required to solve the problem with the tradeoff of a possible miss of a solution in a highly-cluttered environment. Illustrative examples demonstrated the implementation of the methodology in obstacle-free and obstructed spaces.

Appendix A

In this Appendix, it is shown that the equations of the transformed obstacles are analytic and known functions of obstacle parameters and the orientation φ . This facilitates greatly all calculations that are of algebraic nature.

Consider an ellipse with center at (x_0, y_0) and length of principal axes R_a and R_b , rotated by an angle ψ with respect to the x axis. Its parametric equations are

$$x_b(\xi) = x_0 + R_a \cos \xi \cos \psi - R_b \sin \xi \sin \psi \quad (\text{A1})$$

$$y_b(\xi) = y_0 + R_a \cos \xi \sin \psi + R_b \sin \xi \cos \psi, \quad (\text{A2})$$

where $\xi \in [0, 2\pi]$. Substituting eqs (A1) and (A2) into eqs (25) yields

$$\begin{aligned} u_b(\xi) &= u_0 + R_a \cos \xi \sin(\varphi - \psi) \\ &\quad - R_b \sin \xi \cos(\varphi - \psi) \end{aligned} \quad (\text{A3})$$

$$\begin{aligned} v_b(\xi) &= v_0 - R_a \cos \xi \cos(\varphi - \psi) \\ &\quad - R_b \sin \xi \sin(\varphi - \psi). \end{aligned} \quad (\text{A4})$$

Equations (A3) and (A4) describe an ellipse with respect to axes $(u', v') = (u, -v)$ with center at $(u_0, v_0) = (x_0 \sin \varphi - y_0 \cos \varphi, l_G - x_0 \cos \varphi - y_0 \sin \varphi)$, length of principal axes R_a and R_b , which is rotated by $\psi + (\pi/2 - \varphi)$. If we let φ take

values from $[\varphi_{in}, \varphi_{fin}]$ then a family of ellipses is obtained. Each of the ellipses is at a different plane $\varphi = const.$ and has a different orientation while their centers are points on a three dimensional helicoid given by

$$\begin{aligned} \eta(\varphi) &= (u(\varphi), v(\varphi), w(\varphi)) \\ &= (x_0 \sin \varphi - y_0 \cos \varphi, l_G - x_0 \cos \varphi - y_0 \sin \varphi, \varphi). \end{aligned} \tag{A5}$$

The case of a circular obstacle can be derived from an elliptic obstacle, using $R_a = R_b = R$. In this case, ψ becomes irrelevant. The same properties hold and hence a circular obstacle is transformed to a helicoidal tube described by

$$\begin{aligned} \sigma(\varphi, \xi) &= (x_0 \sin \varphi - y_0 \cos \varphi + R \cos \xi, l_G \\ &\quad - x_0 \cos \varphi - y_0 \sin \varphi + R \sin \xi, \varphi), \end{aligned} \tag{A6}$$

where $\varphi \in [\varphi_{in}, \varphi_{fin}]$ and $\xi \in [0, 2\pi]$, while the centers of the circles form a three dimensional helicoid, given by eq (A5).

Appendix B

If α and α' denote the coefficients of the second order polynomials representing the distance from an obstacle for a circular and an elliptic obstacle respectively, see eq (39), then

$$\begin{aligned} \alpha &= (w - w_{fin})^4 (w - w_{in})^4 + 4 (w - w_{fin})^2 \\ &\quad (w - w_{in})^2 (-2w + w_{fin} + w_{in})^2 \end{aligned} \tag{B1}$$

$$\begin{aligned} \alpha' &= (w - w_{fin})^2 (w - w_{in})^2 \\ &\quad \times [R_b^2 ((4w - 2(w_{fin} - w_{in})) \cos(\psi - w) \\ &\quad + (w - w_{fin})(w - w_{in}) \sin(\psi - w))^2 \\ &\quad + R_a^2 ((w - w_{fin})(w - w_{in}) \cos(\psi - w) \\ &\quad + 2(-2w + w_{fin} + w_{in}) \sin(\psi - w))^2]. \end{aligned} \tag{B2}$$

As can be easily seen, both α and α' are non-negative numbers.

As far as eq (46) is concerned, the coefficients are

$$\alpha = 1 \tag{B3}$$

$$\alpha' = R_a^2 \cos^2(\psi - w) + R_b^2 \sin^2(\psi - w). \tag{B4}$$

Finally, the coefficient of the second order monomial in eq (46) is

$$\alpha = -4c_v^2. \tag{B5}$$

The same coefficient for an elliptic obstacle is

$$\alpha' = -4c_v^2 R_a^2 R_b^2, \tag{B6}$$

where c_v is a function of the boundary conditions. It can be easily seen that both α and α' are negative numbers.

Acknowledgments

Support for this work by IRIS III, Canadian Centres of Excellence, (LAW), is gratefully acknowledged. Also, the authors wish to acknowledge the anonymous reviewers for their constructive comments and suggestions.

References

Barraquand, J., and Latombe, J.-C. 1991. Nonholonomic multibody mobile robots: Controllability and motion planning in the presence of obstacles. *Proc. of the IEEE Int. Conf. on Robotics and Automation*, pp. 2328–2335.

Bemporad, A., De Luca, A., and Oriolo, G. 1996. Local incremental planning for a car-like robot navigating among obstacles. *Proc. of the IEEE Int. Conf. on Robotics and Automation*, pp. 1205–1211.

Craig, J. 1989. *Introduction to Robotics, Mechanics and Control*. Addison Wesley.

Divelbiss, A., and Wen, J. 1997. A path space approach to nonholonomic motion planning in the presence of obstacles. *IEEE Tr. on Robotics and Automation* 13(3):443–451.

Ferbach, P. 1995. A method of progressive constraints for nonholonomic motion planning. *IEEE Tr. on Robotics and Automation* 14(1):172–179.

Fleury, S., Soueres, S., Laumond, J.-P., and Chatilla, R. 1995. Primitives for smoothing mobile robot trajectories. *IEEE Tr. on Robotics and Automation* 11(3):441–448.

Fliess, M., Levine, J., Martin, P., and Rouchon, P. 1997. Flatness and defect of nonlinear systems: Introductory theory and examples. *Int. J. of Control* 61(6):1327–1361.

Foulon, G., Fourquet, J.-Y., and Renaud, M. 1998. Planning point to point paths for nonholonomic mobile manipulators. *IEEE/RSJ Int. Conf. on Intelligent Robots and Systems (IROS)*, pp. 374–379.

Foulon, G., Fourquet, J.-Y., and Renaud, M. 1999. Coordinating mobility and manipulation using nonholonomic mobile manipulators. *Control and Engineering Practice*, vol. 7, pp. 391–399.

Gurvitz, L. 1992. Averaging approach to nonholonomic motion planning. *Proc. of the IEEE Int. Conf. on Robotics and Automation*, pp. 2541–2546.

Hootsmans, N. A., and Dubowsky, S. 1991. Large motion control of mobile manipulators including vehicle suspension characteristics. *Proc. of the IEEE Int. Conf. on Robotics and Automation*, pp. 2336–2341.

Ince, E. L. 1956. *Ordinary Differential Equations*. Mineola, NY: Dover Publications.

Jacobs, P., and Canny, J. 1989. Planning smooth paths for mobile robots. *Proc. of the IEEE Int. Conf. on Robotics and Automation*, pp. 2–7.

Kolmanovsky, I., and McClamroch, H. 1995. Developments in nonholonomic control problems. *IEEE Control Systems*, pp. 20–35.

- Lafferriere, G., and Sussmann, H. 1991. Motion planning for controllable systems without drift. *Proc. of the IEEE Int. Conf. on Robotics and Automation*, pp. 1148–1153.
- Laumond, J.-P., Jacobs, J., Taix, M., and Murray, R. M. 1994. A motion planner for nonholonomic mobile robots. *IEEE Tr. on Robotics and Automation* 10(5):577–593.
- Monaco, S., and Normand-Cyrot, D. 1992. An introduction to motion planning under multirate digital control. *Proc. of the IEEE Int. Conf. on Decision and Control*, pp. 1780–1785.
- Murray, R., and Sastry, S. 1993. Nonholonomic motion planning: Steering using sinusoids. *IEEE Transactions on Automatic Control* 38(5):700–716.
- Papadopoulos, E., and Dubowsky, S. 1991. On the nature of control algorithms for free-floating space manipulators. *IEEE Transactions on Robotics and Automation* 7(6):750–758.
- Papadopoulos, E., and Gonthier, Y. 1999. A framework for large-force task planning of mobile redundant manipulators. *J. of Robotic Systems* 16(3):151–162.
- Papadopoulos, E., and Poulakakis, J. 2000a. On motion planning of nonholonomic mobile robots. *Int. Symposium of Robotics*, pp. 77–82.
- Papadopoulos, E., and Poulakakis, J. 2000b. Planning and model-based control for mobile manipulators. *IEEE/RSJ Int. Conf. on Intelligent Robots and Systems (IROS)*, pp. 1810–1815.
- Papadopoulos, E., and Rey, D. 1996. A new measure of tipover stability margin for mobile manipulators. *Proc. of the IEEE Int. Conf. on Robotics and Automation*, pp. 3111–3116.
- Pars, L. A. 1965. *A Treatise on Analytical Dynamics*. New York: Wiley & Sons.
- Perrier, C., Dauchez, P., and Pierrot, F. 1998. A global approach for motion generation of non-holonomic mobile manipulators. *Proc. of the IEEE Int. Conf. on Robotics and Automation*, pp. 2971–2976.
- Scheuer, S., and Fraichard, Th. 1997. Collision-free and continuous-curvature path planning for car-like robots. *Proc. of the IEEE Int. Conf. on Robotics and Automation*, pp. 867–873.
- Sekhavat, S., and Laumond, J.-P. 1998. Topological property for collision-free nonholonomic motion planning: The case of sinusoidal inputs for chained form systems. *IEEE Tr. on Robotics and Automation* 14(5):671–680.
- Seraji, H. 1998. A unified approach to motion control of mobile manipulators. *The Int. J. of Robotics Research* 17(2):107–118.
- Shiller, Z. 2000. Obstacle traversal for space exploration. *Proc. of the IEEE Int. Conf. on Robotics and Automation*, pp. 989–994.
- Shkel, A. M., and Lumelsky, V. 1997. Curvature-constrained motion within a limited workspace. *Proc. of the IEEE Int. Conf. on Robotics and Automation*, pp. 1394–1399.
- Svestka, P., and Overmars, M. 1994. Motion planning for car-like robots using a probabilistic learning approach. Technical Report UU-CS-1994-33, Utrecht University.
- Tanner, H., and Kyriakopoulos, K. 2000. Nonholonomic motion planning for mobile manipulators. *Proc. of the IEEE Int. Conf. on Robotics and Automation*, pp. 1233–1238.
- Wiens, G. J. 1989. Effects of dynamic coupling in mobile robotics systems. *Proc. of the ASME Robotics Research World Conference*, pp. 3-43–3-53.
- Yamamoto, Y., and Yun, X. 1995. Coordinated obstacle avoidance of a mobile manipulator. *Proc. of the IEEE Int. Conf. on Robotics and Automation*, pp. 2255–2260.